

Cardiac-specific overexpression of the human type 1 angiotensin II receptor causes delayed repolarization

Katy Rivard^{1,2}, Pierre Paradis^{3,†}, Mona Nemer³, and Céline Fiset^{1,2,*}

¹Research Centre, Montreal Heart Institute, 5000 Rue Bélanger, Montréal, QC, Canada H1T 1C8; ²Université de Montréal, Faculty of Pharmacy, Montréal, QC, Canada; and ³Institut de Recherche Clinique de Montréal, Montréal, QC, Canada

Received 8 December 2007; revised 8 January 2008; accepted 11 January 2008; online publish-ahead-of-print 31 January 2008

Time for primary review: 41 days

KEYWORDS

Angiotensin II;
K⁺ currents;
Ventricular repolarization;
Arrhythmias;
Transgenic mice

Aims Mice with cardiac-specific overexpression of human angiotensin II type 1 receptor (AT1R) undergo cardiac remodelling and die prematurely of sudden death. Since excessive QT prolongation is a major risk factor for ventricular arrhythmias and sudden death, we hypothesize that chronic stimulation of AT1R might contribute to sudden death by promoting delayed repolarization and ventricular arrhythmias.

Methods In the present study, a detailed analysis of ventricular repolarization parameters was undertaken in AT1R mice.

Results Measurement of K⁺ currents in ventricular myocytes isolated from 6–8 months AT1R male mice revealed a significant reduction of the Ca²⁺-independent transient outward (*I*_{to}), the ultra-rapid delayed rectifier (*I*_{Kur}), and the inward rectifier (*I*_{K1}) K⁺ currents compared with littermate controls (CTL). The expression of the underlying K⁺ channels was also decreased in AT1R ventricles. Moreover, reactivation of *I*_{to} was slower in AT1R mice. Consistent with these findings, AT1R mice presented a longer action potential duration (APD₉₀, CTL: 19.0 ± 1.8 ms; AT1R: 39.1 ± 4.7 ms, *P* = 0.0001) and QTc interval (CTL: 53.6 ± 1.5 ms, AT1R: 64.2 ± 1.4 ms, *P* = 0.0005). In addition, spontaneous ventricular arrhythmias were reported in the AT1R mice. Importantly, the increased incidence of arrhythmia and the repolarization defects also occurred in much younger AT1R mice that do not present signs of hypertrophy, confirming that these arrhythmogenic changes are not secondary to cardiac remodelling.

Conclusion These results strongly suggest that chronic stimulation of AT1R directly leads to an increased incidence of cardiac arrhythmia associated with delayed repolarization.

1. Introduction

Angiotensin II (ANG II), the active end product of the renin–angiotensin system (RAS), has numerous physiological effects on the cardiovascular system. Unfortunately, under pathological conditions, the increased activity of RAS contributes to the development of ventricular hypertrophy and remodelling.^{1–5} To date, most of the cardiac damaging effects of ANG II appear to be mediated by the ANG II type 1 receptor (AT1R).⁶ Although it is well recognized that ANG II is involved in the initiation of cardiac remodelling,^{7–10} relatively little is known concerning the role of ANG II in the higher propensity of lethal cardiac arrhythmias associated with heart disease.^{4,5,11} Activity of the RAS appears to be able to alter repolarization in myocardium.¹² However, while transgenic mouse models with cardiac restricted overexpression of different components of the RAS have been

instrumental in studying the role of ANG II in cardiac remodelling,^{10,13,14} no detailed characterization of cardiac cellular excitability has been realized using these genetically manipulated mouse models. Thus far, only a small number of studies have documented an increased incidence of cardiac arrhythmias and sudden death in these transgenic mice.^{15–17} Blockade of AT1R (AT1R antagonist, ARA) has been shown to decrease the arrhythmia morbidity in mice with ventricular hypertrophy.⁴ In addition, angiotensin-converting enzyme inhibitors (ACEI) have been reported to restore normal ventricular action potential duration (APD), refractoriness, and reduced susceptibility to ventricular fibrillation.⁵ Recently, using transgenic mice with cardiac-specific ANG II overproduction, Domenighetti *et al.*¹³ reported an increased incidence of ventricular arrhythmias and QT interval prolongation associated with a reduced density of inward rectifier K⁺ current in mouse. However, they did not examine any of the other K⁺ currents/channels involved in mouse ventricular repolarization.

Transgenic mice overexpressing the human AT1Rs specifically in cardiomyocytes have been shown to develop

[†] Present address: Lady Davis Institute for Medical Research, Jewish General Hospital, Montreal.

* Corresponding author. Tel: +1 514 376 3330 (3025); fax: +1 514 376 1355.
E-mail address: celine.fiset@icm-mhi.org

hypertrophy and heart failure in the absence of hypertension.¹⁰ Moreover, these AT1R mice die prematurely and spontaneously, suggesting that under pathological conditions, ANG II might contribute to cardiac sudden death by promoting severe cardiac arrhythmias. Since excessive QT prolongation, which reflects delayed repolarization, is a major risk factor for ventricular arrhythmias and sudden death, we conducted the present study to determine whether there was a causal relationship between chronic AT1R activation, delayed repolarization, and cardiac arrhythmias. Findings presented here reveal that overexpression of the AT1R in the myocardium leads to delayed repolarization which could contribute to the increased incidence of cardiac arrhythmia.

2. Methods

A detailed description of all the following methods used in this study can be found in the online data supplement.

2.1 Animals

Experiments were performed on male C57BL/6 AT1R mice aged of either 6–8 months or 50 ± 5 days. This transgenic mouse model overexpressing the human AT1R receptor (200-fold in the ventricles of the transgenic mice of both age groups) specifically in cardiomyocytes was described previously.¹⁰ Heterozygous transgenic mice (AT1R) and age-matched wild-type littermates (CTL) were used. All experiments were conducted in accordance with the Canadian Council Animal Care guidelines and conformed to the Guide for the Care and Use of Laboratory Animals published by the US National Institutes of Health (NIH Publication No. 85–23, revised 1996).

2.2 Ventricular myocyte isolation

The ventricular myocyte isolation protocol has been described previously.¹⁸

2.3 Electrophysiology

2.3.1 Cellular electrophysiology

All experiments were carried out at room temperature (20–22°C). The whole-cell voltage- and current-clamp recording methods, data acquisition, voltage-clamp protocols, and analysis methods have been described previously.¹⁹

2.3.2 Surface ECG

Mice were anaesthetized with isoflurane. Electrodes were placed subcutaneous and surface ECG were acquired in lead I configuration. The QT intervals were corrected (QTc) for the heart rate using the formula for mice ($QTc = QT / (RR/100)^{1/2}$).²⁰

2.3.3 Telemetry recording

Telemetry was used to record spontaneous ventricular arrhythmias in conscious free moving unanaesthetized CTL and AT1R mice. ECG lead placement represented lead II configuration.

2.4 Western blots analysis

Protocols used for isolation of sarcolemmal-enriched protein and Western blot analysis were identical to those reported previously.^{18,21}

2.5 Real-time PCR

RNA levels of the different K⁺ channels (Kv1.5, Kv2.1, Kv4.2, KChIP2, and Kir2.1) were determined by real-time PCR as described

previously.²² mRNA expression was quantified relative to cyclophilin.

2.6 Echocardiography

Echocardiography was performed as described previously.²³ This was done to determine the left ventricular internal dimension in systole and diastole (LVIDs and LVIDd, respectively) and the fractional shortening (FS).

2.7 Statistical analysis

Results are expressed as mean \pm SEM. An unpaired Student's *t*-test was used to compare means. *P*-value of <0.05 was considered significant.

3. Results

3.1 Alteration of K⁺ currents in 6–8 months AT1R mouse ventricular myocytes

Figure 1A shows that the total K⁺ current (I_{peak}) was significantly smaller in AT1R myocytes compared with CTL cells (at +30 mV, CTL = 68.1 ± 9.2 pA/pF and AT1R = 28.2 ± 4.6 pA/pF; *P* = 0.001). The individual K⁺ conductance contributing to I_{peak} in mouse ventricular tissue were then compared. These K⁺ currents correspond to (i) the Ca²⁺-independent transient outward (I_{to}), (ii) the ultra-rapid delayed rectifier (I_{Kur}), (iii) the steady-state outward (I_{ss}), and (iv) the inward rectifier (I_{K1}) K⁺ currents.¹⁹ Mean current-voltage (*I*-*V*) relationships (Figure 1B) show a significant decrease of I_{to} in AT1R cells compared with CTL myocytes (at +30 mV, CTL = 31.9 ± 3.9 pA/pF and AT1R = 9.8 ± 1.4 pA/pF; *P* = 0.00004). As shown in Figure 1C, I_{Kur} also was significantly decreased in AT1R mice (at +30 mV, CTL = 27.3 ± 5.5 pA/pF and AT1R = 9.8 ± 1.4 pA/pF; *P* = 0.04). In contrast, the third component of the outward K⁺ current, I_{ss} , was similar in both groups (*P* = NS) (Figure 1D). Figure 1A and D also presents data on I_{K1} . The inward portion of I_{K1} was significantly smaller in AT1R myocytes compared with CTL cells (at -110 mV, CTL = -21.3 ± 1.2 pA/pF and AT1R = -11.9 ± 1.1 pA/pF, *P* = 0.00009). The outward part of I_{K1} (-80 to -40 mV) was also significantly decreased in AT1R myocytes (at -60 mV, CTL = 1.6 ± 0.2 pA/pF and AT1R = 0.9 ± 0.1 pA/pF, *P* = 0.003).

Figure 2A compares the voltage dependence of steady-state inactivation of I_{to} in CTL and AT1R ventricular myocytes. The right panel presents Boltzmann functions fitted to mean data. The steady-state inactivation of I_{to} was similar in both groups ($V_{1/2}$, CTL = -53.2 ± 0.7 mV; AT1R = -52.4 ± 0.7 mV, *P* = 0.3; slope factor (*k*), CTL = 5.9 ± 0.5 mV; AT1R = 7.3 ± 0.8 mV, *P* = 0.2). Figure 2B shows the recovery from inactivation of I_{to} in AT1R mice. Examples of the family of currents that illustrate the time course of recovery at -80 mV for CTL and AT1R myocytes are shown in the left panel. The recovery from inactivation was significantly slower in AT1R myocytes (time constant: 79 ± 7 ms) compared with controls (34 ± 2 ms) (*P* = 0.000001).

We also studied the steady-state inactivation and the recovery from inactivation of I_{Kur} in AT1R mice. The voltage dependence of steady-state inactivation of I_{Kur} was comparable in CTL (*n* = 12) and AT1R (*n* = 6) cardiomyocytes ($V_{1/2}$, CTL = -41.4 ± 1.1 mV and AT1R = -41.1 ± 1.1 mV, *P* = 0.9; *k*, CTL = 6.0 ± 0.4 mV and AT1R = 6.2 ± 1.0 mV, *P* = 0.9). The recovery from inactivation of I_{Kur} was also comparable in

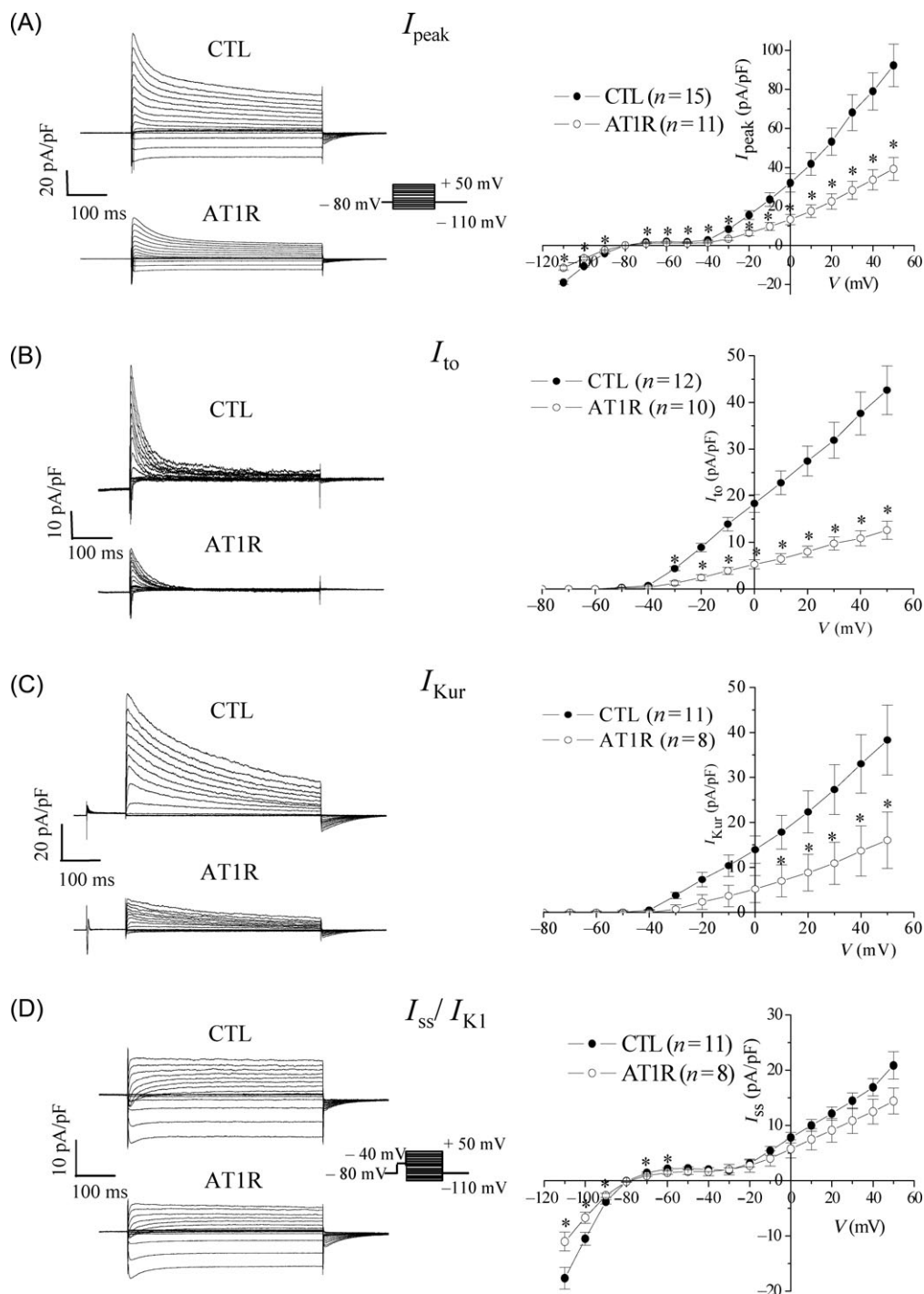


Figure 1 K^+ currents in 6–8 months AT1R ventricular mouse myocytes. (A) The total K^+ current (I_{peak}). Left: representative family of I_{peak} recorded from CTL and AT1R ventricular myocytes using the protocol shown in inset. Right: comparison of mean I - V curves for I_{peak} ($*P < 0.05$). (B) I_{to} —left. Superimposed current records corresponding to I_{to} calculated by subtraction of current traces recorded with and without an inactivating prepulse (100 ms, -40 mV) applied before the main activation steps (protocol shown in inset, D).¹⁹ Right: mean I - V curves for I_{to} ($*P < 0.05$). (C) I_{Kur} —left. After inactivation of I_{to} the remaining outward current (recorded with the protocol shown in inset, D) is composed of I_{Kur} and I_{ss} and can be separated with $100 \mu\text{M}$ of 4-aminopyridine (4-AP). Family of membrane currents presented in the left panel represents I_{Kur} (the 4-AP-sensitive component) in CTL and AT1R cells. Right: corresponding mean I - V curves for I_{Kur} ($*P < 0.05$). (D) I_{ss} and I_{K1} —left. Typical examples of I_{K1} and the 4-AP resistant component of the outward current, I_{ss} , recorded in CTL and AT1R myocytes. Right: corresponding I - V curves for I_{K1} and I_{ss} showing that I_{K1} was significantly reduced in AT1R mice ($*P < 0.05$), whereas I_{ss} was similar in CTL and AT1R myocytes. Electrophysiological protocols used to record the different K^+ currents are described in the Supplementary material.

CTL and AT1R myocytes, with a time constant of 552 ± 59 ms in CTL ($n = 12$) and 490 ± 33 ms in AT1R ($n = 9$) ($P = 0.4$). These results indicate that the reduced I_{Kur} density observed in AT1R ventricular myocytes cannot be explained by an alteration in I_{Kur} inactivation kinetic properties.

3.2 Changes in K^+ channels expression in AT1R mouse ventricle

Using Western blot analysis, we compared the protein expression levels of the K^+ channels (Kv1.5, Kv2.1, Kv4.2/

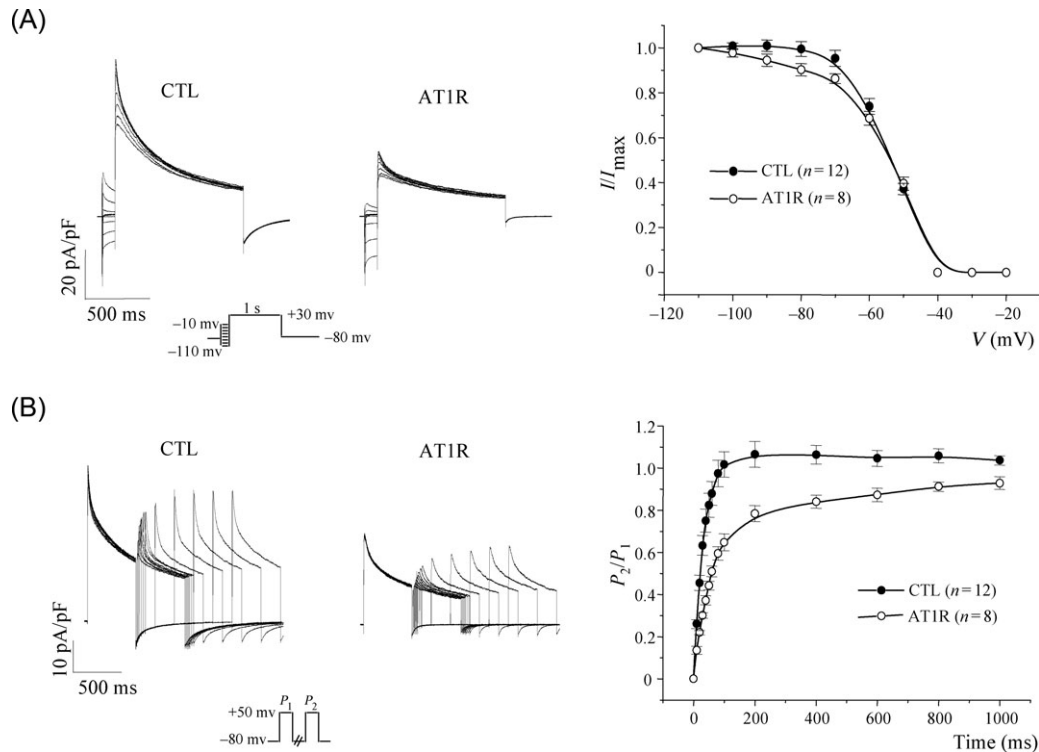


Figure 2 Steady-state inactivation and reactivation of I_{to} in 6–8 months AT1R ventricular mouse myocytes. (A) Voltage dependence of steady-state inactivation of I_{to} . Left: typical examples of family of currents. Right: plot of voltage dependence of the steady-state inactivation of I_{to} . The amplitude of I_{to} for each pre-pulse membrane potential was determined by subtracting each test pulse current with that obtained with the -40 mV pre-pulse. The I_{to} test pulse amplitude was normalized to the amplitude at the most negative pre-pulse potential (I/I_{max}). (B) Reactivation of I_{to} . Left: example of family of membrane currents showing the time course of recovery of I_{to} from inactivation. A 500 ms inactivating pulse ($+50$ mV) was followed at intervals of 10, 20, 30, 40, 50, 60, 80, 100, 200, 400, and 600 ms by an identical test pulse. Right: membrane potential dependence of recovery from inactivation of I_{to} . P_2/P_1 is the ratio of test pulse current/pre-pulse current amplitudes. I_{to} amplitude was measured as the difference between peak outward current and the current 150 ms after the peak. The smooth lines are best-fit single exponential functions.

Kv4.3, and Kir2.1) corresponding to the murine ventricular K^+ currents (I_{Kur} , I_{ss} , I_{to} , and I_{K1} , respectively).^{24–27} In line with the electrophysiological data, protein expression of Kv1.5, Kv4.2, and Kir2.1 was decreased in AT1R ventricle compared with CTL (Figure 3A). However, Kv4.3 protein expression was similar in the two groups, whereas Kv2.1 was increased in AT1R ventricle compared with controls.

To determine whether the changes observed in the protein level could be explained by transcriptional or post-transcriptional mechanisms, real-time PCR analysis was carried out on the K^+ channel isoforms that exhibit differences at the protein level. Since both density and voltage-dependent kinetics of recovery from inactivation of I_{to} can also be influenced by the expression of the KChIP2 ancillary subunit, we also determined whether the transcript level of KChIP2 was affected by the AT1R overexpression. In support of a transcriptional regulation for Kv4.2 and KChIP2, the real-time PCR experiments revealed a significant reduction of Kv4.2 and KChIP2 mRNA transcripts in AT1R compared with CTL ventricles. In contrast, the mRNA levels for Kv1.5, Kv2.1, and Kir2.1 were similar between the two groups (Figure 3B), suggesting a post-transcription mechanism of regulation for these subunits.

3.3 Physiological implication of the decrease of the K^+ currents in AT1R mice

Consistent with the decrease of the K^+ currents in AT1R ventricles, APD was significantly longer in AT1R myocytes

compared with those measured in CTL myocytes (in ms) (APD₂₀, CTL = 2.5 ± 0.2 ; AT1R = 4.3 ± 0.3 , $P = 0.00006$), (APD₅₀, CTL = 5.2 ± 0.9 ; AT1R = 9.7 ± 1.2 , $P = 0.007$), (APD₉₀, CTL = 19.0 ± 1.8 ; AT1R = 39.1 ± 4.7 , $P = 0.0005$) (Figure 4A). Moreover, in keeping with the prolongation of the ventricular APDs, both QT and QTc intervals were significantly prolonged in AT1R compared with CTL mice (Figure 4B). However, heart rate was comparable between both groups. Of note, the QRS complex and the QRS corrected for the heart rate (QRS_c) were significantly longer in the AT1R mice. However, even after subtracting the QRS (or QRS_c) from the QT (or QTc), the prolongation was still statistically significant (respectively, $P = 0.02$ and 0.01) (Figure 4B), confirming that the repolarization process is markedly delayed in the AT1R mice.

ECG recordings have been obtained using a telemetry system on free moving CTL and AT1R mice to determine whether the overexpression of the AT1R was associated with spontaneous arrhythmias. Figure 4C illustrates typical examples of ECG traces recorded from control (a) and AT1R (b–c) mice aged 6–8 months. While none of the six CTL mice experienced rhythm abnormalities, a mixture of spontaneous ventricular arrhythmias was observed in AT1R mice. The examples presented in Figure 4C illustrate different irregular rhythms observed in AT1R mutant mice: a polymorphic ventricular arrhythmia and a normal sinus rhythm interrupted by episodes of irregular rhythm with wider QRS complexes. Similar arrhythmia episodes have been observed in five out of six AT1R mice.

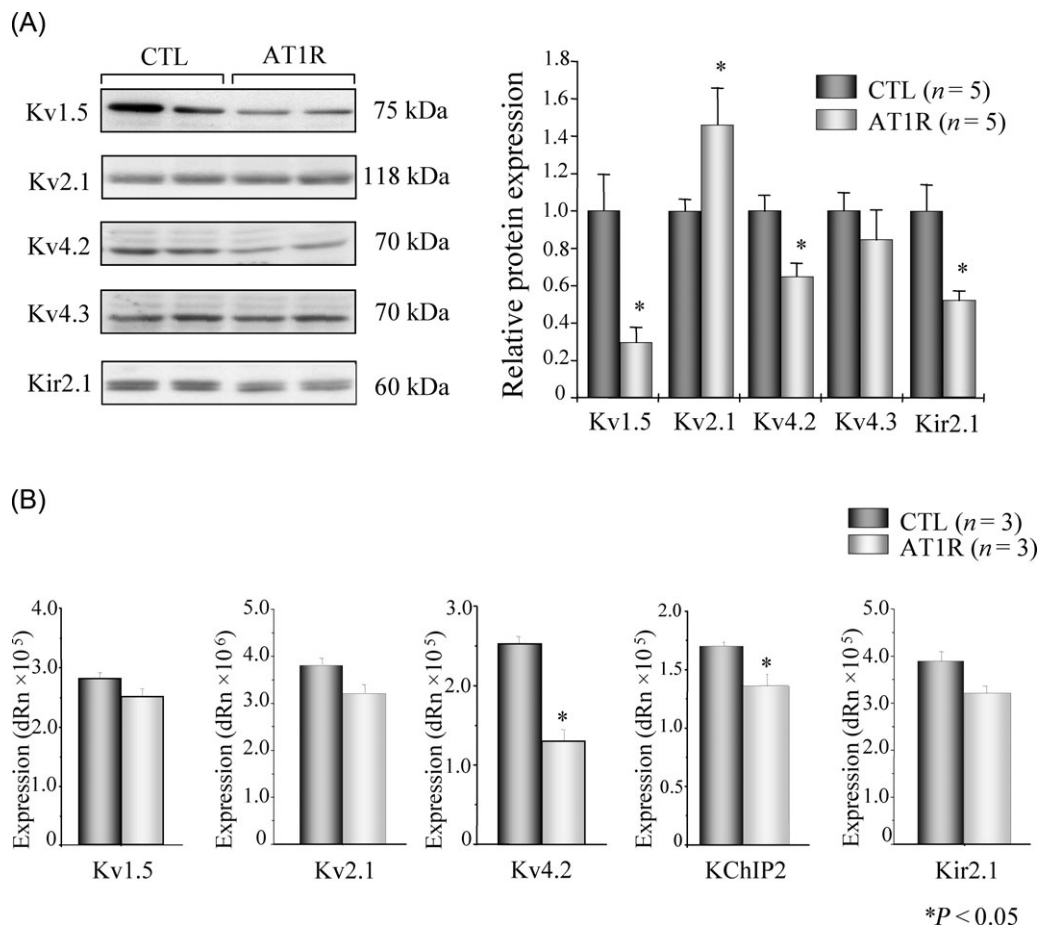


Figure 3 K^+ channel expression in 6–8 months AT1R mouse ventricles. (A) Protein expression of K^+ channels. Western blot analysis of Kv1.5 (1:500), Kv2.1 (1:500), Kv4.2 (1:1000), Kv4.3 (1:5000), and Kir2.1 (1:500) on sarcolemmal-enriched fraction (100 μ g/lane, one ventricle/sample) isolated from CTL and AT1R ventricle. Equal protein loading was confirmed by ponceau-S stained membranes. Bar graph (right) represents relative protein expression of the K^+ channels determined by densitometry. Relative abundance was calculated with the value of CTL as a reference of 100% (* $P < 0.05$). (B) mRNA expression of K^+ channels. Bar graph comparing the abundance of Kv1.5, Kv2.1, Kv4.2, KChIP2, and Kir2.1 mRNA transcripts in CTL and AT1R mice determined by real-time PCR. Each sample was analysed in triplicate (* $P < 0.05$).

These arrhythmias were seen throughout the 24 h recording period.

3.4 Cardiac remodelling in 6–8 months AT1R mice

A common electrical alteration present in heart diseases is the prolongation of APD,^{28–30} a known risk factor for severe ventricular arrhythmias. Thus, it was important to determine whether the arrhythmogenic changes described in the AT1R mice were the result of alterations in the context of cardiac remodelling or a direct consequence of chronic AT1 stimulation. To address this question, young adult mice (50 \pm 5 days) also were studied. We first examined cardiac structure and function of these AT1R mice. The results showed that compared with CTL, the 6–8 months AT1R mice exhibit an increased left ventricular mass (LV_{mass}) to body weight (BW) ratio [LV_{mass}/BW (mg/g), CTL: 3.39 \pm 0.20; AT1R: 4.26 \pm 0.25; $P = 0.01$] (Figure 5A). Cell capacitances (an indication of cell volume) of ventricular myocytes also were larger in AT1R mice (CTL: 162.8 \pm 8.5 pF; AT1R: 216.4 \pm 23.5 pF; $P = 0.01$) (Figure 5B). Thus, these data indicate that the hearts from AT1R mice exhibit hypertrophy. Using ventricular internal dimensions in systole and diastole (determined by

echocardiography), the FS was calculated. A significant reduction of this marker of cardiac function was observed in AT1R hearts (CTL: 55.6 \pm 0.9%; AT1R: 27.4 \pm 1.3%, $P < 0.00001$) (Figure 5C and D). Taken together, these data demonstrate that there was clear evidence of both cardiac hypertrophy and failure in 6–8 months AT1R mice.

3.5 Ventricular repolarization defects and cardiac arrhythmias in younger AT1R mice

To ascertain that the repolarization defects seen in AT1R mice were not secondary to cardiac hypertrophy or failure, we characterized ventricular repolarization in much younger AT1R mice (50 \pm 5 days) that have similar AT1R expression as 6–8 months AT1R mice, but do not present cardiac remodelling. Capacitance of the ventricular myocytes of these young AT1R mice was comparable with that of age-matched littermate controls (CTL: 149.2 \pm 6.9 pF, $n = 20$; AT1R: 139.5 \pm 8.0 pF, $n = 19$, $P = 0.4$) further confirming the absence of hypertrophy at the cellular level. The results presented in Figure 6 indicate that the younger transgenic mice exhibit a repolarization defect similar to that observed in the 6–8 months AT1R mice. Indeed, compared with their age-matched controls, the

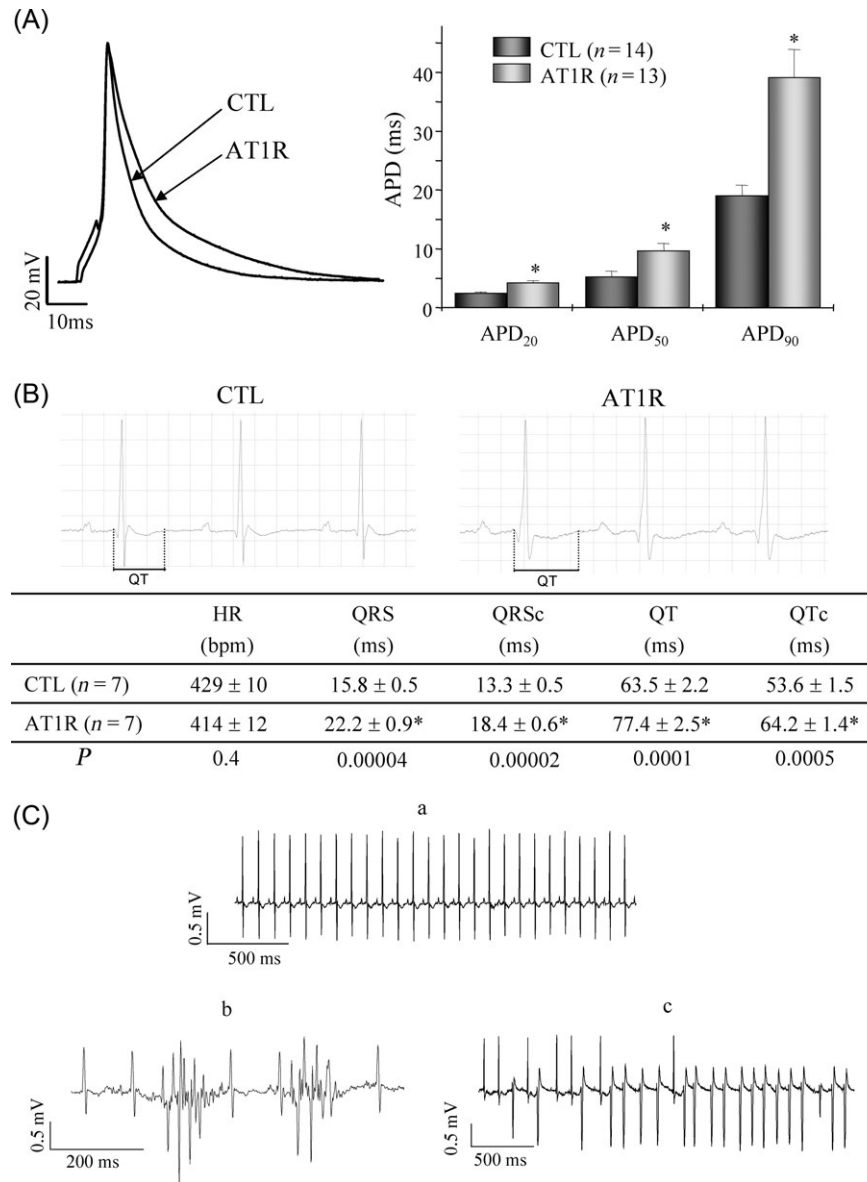


Figure 4 Ventricular repolarization and cardiac rhythm in 6–8 months AT1R mice. (A) Comparison of APDs between CTL and AT1R mice. Left: typical examples of AP recorded at 4 Hz. Bar graph (right) shows mean APD₂₀, APD₅₀, and APD₉₀ (± SEM) (**P* < 0.01). (B) Table comparing mean values for ECG parameters between CTL and AT1R mice obtained with surface ECG recordings. (C) Representative ECG recordings obtained with telemetry monitoring in CTL and AT1R mice. These examples illustrate polymorphic (b) and monomorphic (c) irregular rhythms observed in two AT1R mice, whereas no rhythm abnormalities were recorded in CTL (a).

50 days AT1R mice had longer QTc interval (CTL: 46.0 ± 1.4 ms; AT1R: 56.9 ± 2.1 ms, *P* = 0.0004) and APD (APD₂₀, CTL: 2.2 ± 0.1 ms; AT1R: 4.2 ± 0.3 ms, *P* < 0.00005), (APD₅₀ CTL: 4.2 ± 0.2 ms; AT1R: 12.1 ± 1.4 ms, *P* < 0.00005), (APD₉₀, CTL: 16.7 ± 0.8 ms; AT1R: 34.9 ± 3.1 ms, *P* < 0.00005) (Figure 6A and B). In addition, 50 days AT1R mice exhibited a decrease in density of the outward component of *I*_{peak} (at +30 mV; CTL: 64.2 pA/pF and AT1R: 28.4 ± 3.1 pA/pF, *P* < 0.00001). Of note, this reduction was similar to that observed in 6–8 months AT1R mice (Figure 6C). Similar to what was seen in the older group, the 50 days AT1R mice also had a reduced density of *I*_{to} and *I*_{Kur} compared with their age-matched control counterparts (Figure 6D). However, *I*_{ss} was decreased in 50 days AT1R (at +30 mV, CTL: 14.8 ± 0.7 pA/pF and AT1R: 11.3 ± 0.8 pA/pF, *P* = 0.002), but *I*_{K1} was similar (at -110 mV,

CTL = -19.7 ± 1.4 pA/pF and AT1R = -18.0 ± 1.0 pA/pF, *P* = 0.3).

Telemetry monitoring of young AT1R mice revealed that these electrophysiological defects were associated with a variety of spontaneous arrhythmias in three out of three young AT1R mice tested (data not shown). These arrhythmias were similar to those observed in the older AT1R animals. In contrast, no arrhythmias were observed in age-matched littermate CTL (zero out of four).

4. Discussion

The present work provides important new insight into the electrical remodelling that occurs as a consequence of chronic stimulation of myocardial AT1R. First, our results obtained in a mouse model of cardiac-specific

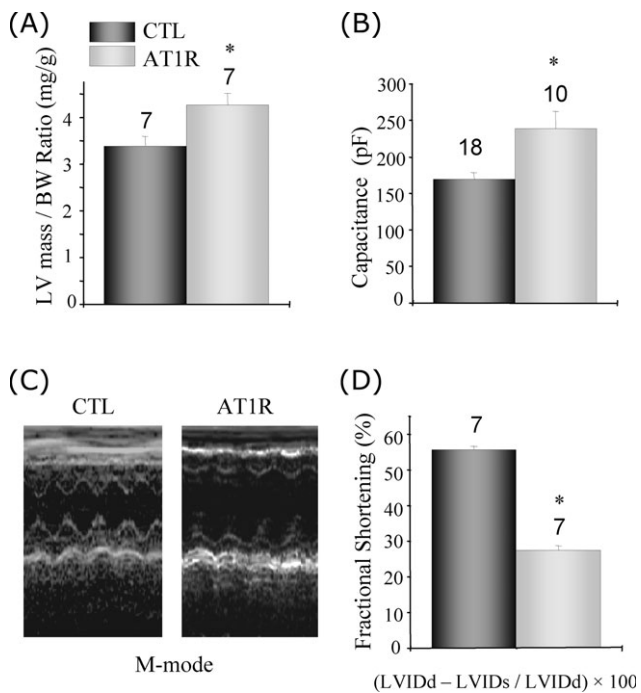


Figure 5 Cardiac function in 6–8 months AT1R mice. (A) Bar graph compares the left ventricular mass (LV mass) corrected for body weight (BW) between CTL and AT1R ($P = 0.01$). (B) Comparison of the cell capacitance measured in CTL and AT1R ventricular myocytes ($P = 0.01$). (C) Typical example of an M-mode echocardiography used to calculate the fractional shortening. (D) Left ventricular fractional shortening = $(LVIDd - LVIDs) / LVIDd \times 100$ ($P < 0.00001$).

overexpression of human AT1R revealed the occurrence of ventricular arrhythmias and the electrophysiological consequences of AT1 overexpression. We found prolonged APD, delayed repolarization, and alterations in several K^+ currents/channels. Secondly, studies in younger mice, prior to the development of overt cellular hypertrophy, indicate that these electrical changes precede the anatomic disturbances, suggesting that the arrhythmogenic changes do not occur as a consequence of cardiac remodelling, but are directly associated with overstimulation of the AT1R. Thirdly, the electrophysiological alterations described here also occur independently of haemodynamic changes,¹⁰ ruling out the involvement of peripheral vascular changes in the phenotype observed.

In both age groups, the QTc interval and APD were significantly prolonged in the AT1R mice. The K^+ currents affected in the older AT1R mice were I_{to} , I_{Kur} , and I_{K1} , whereas those affected in the younger animals were I_{to} , I_{Kur} , and I_{ss} . The fact that I_{ss} was reduced in the 50 days AT1R mice implies that this current is affected by chronic stimulation of the AT1R. However, in the older group, I_{ss} was similar between CTL and AT1R mice. It is possible that the density of I_{ss} increases with time to compensate the reduction of the other outward K^+ currents. Compensatory upregulation of Kv2.1 (I_{ss}) has been reported in previous studies.^{31,32} Indeed, following targeted replacement of Kv1.5, RNA and protein of Kv1.5 were undetectable and Kv2.1 protein was increased in a transgenic model of delayed repolarization.^{31,32} In the present study, the increased Kv2.1 protein expression seen in the older AT1R mice also supports a time-

dependent compensatory upregulation of Kv2.1. Furthermore, because I_{ss} does not contribute as much as I_{to} or I_{Kur} at the peak of the total K^+ current, the difference in the density of I_{ss} in AT1R mice between 50 days and 6–8 months mice is not sufficient to result in a significant change in the amplitude of I_{peak} .

The other noticeable difference between the younger and older AT1R mice relates to I_{K1} . In the 6–8 months AT1R myocytes, I_{K1} was smaller compared with the controls. In contrast, in the younger AT1R mice, I_{K1} was not altered. The fact that younger and older AT1R mice display a similar density of AT1R implies that the difference between the two age groups is not due to the degree of overexpression. In fact, the I_{K1} data strongly suggest that changes in the density of this K^+ current in the older AT1R mice might result from alterations in intracellular signalling associated with cardiac hypertrophy and would not be directly due to the increase stimulation of AT1R. In a separate study, we observed that overexpression of wild-type α_{1B} -adrenergic receptor (α_{1B} -AR) in mice did not affect the density of I_{K1} (unpublished data, Rivard *et al.*, 2008). Of note, the late-onset heart failure phenotype observed in α_{1B} -AR mice was not preceded by longstanding cardiac hypertrophy. Taken together these findings suggest that I_{K1} might be altered only in the presence of hypertrophy.

In a recent study, Domenighetti *et al.*¹³ studied 50–60 weeks transgenic mice with cardiac-specific ANG II overproduction. They reported that these mice develop hypertrophy associated with prolonged QT interval and APD. These observations were attributed to a decrease in I_{K1} , which was the only current examined in their study. A reduction of I_{K1} in that model of hypertrophy would agree with a relationship between downregulation of I_{K1} and the presence of cardiac remodelling. However, although they reported that the animals studied presented ventricular hypertrophy, they failed to establish a correlation between cell capacitance and the density of I_{K1} . Based on that observation, they concluded that the reduction of I_{K1} was independent of cell size and hypertrophy. However, to clearly establish the contribution of hypertrophy on I_{K1} density it would have been more informative to test younger animals that do not present signs of hypertrophy.

The results obtained in our expression studies indicate the chronic stimulation of the AT1R decreased I_{to} density and altered its kinetics of reactivation through alteration of Kv4.2 and KCHIP2 transcription. However, Kv4.3 expression levels were unaffected in AT1R mice. We also observed that overexpression of α_{1B} -AR in mouse heart decreased I_{to} , Kv4.2 and KCHIP2 without any effect on Kv4.3 (unpublished data). Our expression studies also suggest that the decreased density of I_{Kur} and I_{K1} observed in the AT1R mice could be explained by post-transcriptional regulation as suggested by decreased protein expression of Kv1.5 (I_{Kur}) and Kir2.1 (I_{K1}) without changes in the mRNA levels.

Fischer *et al.*³³ have recently reported that hypertensive transgenic rats harbouring the human renin and angiotensinogen genes developed cardiac damage leading to sudden death. They also observed that ventricular tachycardia was common in these animals. Although they did not have any cellular electrophysiological data, they used non-invasive cardiac magnetic field mapping to report that depolarization and repolarization were prolonged and inhomogeneous. These data are in strong support of the findings reported

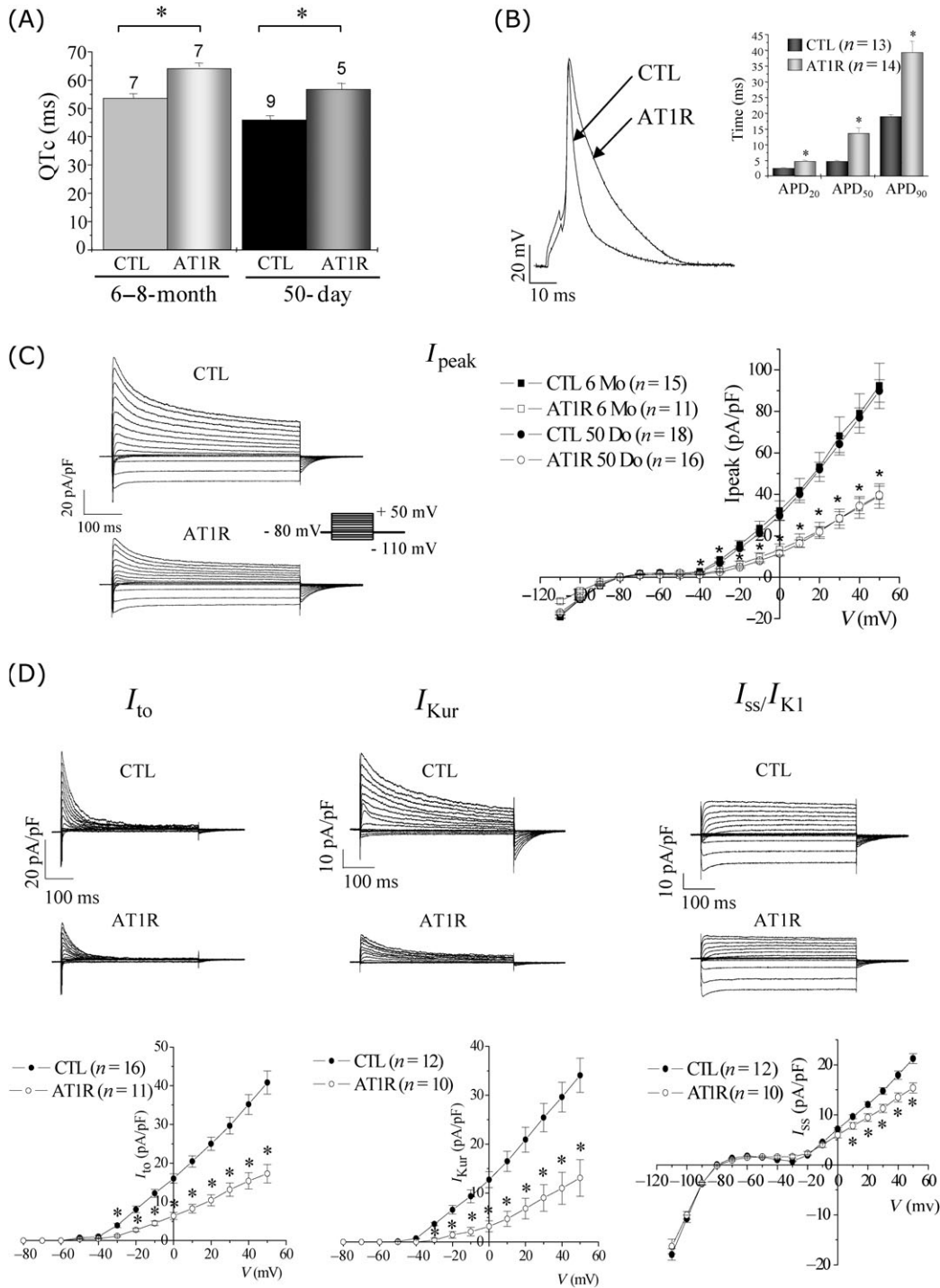


Figure 6 Comparison of the ventricular repolarization phenotype between 6–8 months (6 Mo) and 50 days (50 Do) AT1R male mice. **(A)** Comparison of the QTc interval between the CTL and AT1R mice at 50 days and 6–8 months ($*P < 0.05$). **(B)** Comparison of APD between 50 days CTL and AT1R mice. Typical examples of AP recorded at 4 Hz are presented. Bar graph presents mean APD (\pm SEM) ($*P < 0.05$). **(C)** Comparison of I_{peak} in CTL and AT1R at 6–8 months and 50 days mice. Left: typical examples of I_{peak} recorded in CTL and AT1R myocytes at 50 days. Right: mean $I-V$ curves obtained in CTL and AT1R mice in the two age groups. (square: 6–8 months mice, circle: 50 days mice) ($*P < 0.05$ for young AT1R group). **(D)** Comparison of individual K^+ currents in 50 days CTL and AT1R mice. Representative family of currents (top) and comparison of mean I/V curve between CTL and AT1R myocytes (bottom) for I_{to} , I_{Kur} , and I_{ss}/I_{K1} are presented ($*P < 0.05$).

here. However, because of the presence of hypertension in that rat model, it is hard to determine whether the observed electrical remodelling occurs as a consequence of ANG II stimulation or results from hypertension.

Our results are also consistent with previous reports showing a relationship between ANG II and ionic currents.

In vascular smooth muscle cells, ANG II has been shown to inhibit several K^+ channels, including K_{ATP} , B_{KCa} , and Kv channels.^{34–36} Similarly, different groups have reported that cardiac K^+ currents are attenuated after application of ANG II.^{37–39} Furthermore, in some studies, the effects of ANG II on ionic currents could be reversed when the action

of ANG II was blocked with ACEI or ARA.³⁹ Findings reported here also agree with previous reports showing beneficial effects of ACEI or ARA in preventing arrhythmic mortality.^{4,5}

The primary objective of the telemetry experiments was to detect spontaneous arrhythmias and nearly all AT1R mice studied (eight out of nine; old and young AT1R mice altogether) exhibited spontaneous cardiac arrhythmias during the telemetry monitoring. However, none of these mice died during the 24 h recording period. Clearly, that recording time was sufficient to detect spontaneous arrhythmias; however, a much longer recording period would be necessary to obtain ECG evidence for spontaneous sudden death events.

Taken together the association of ventricular repolarization defects with the increased incidence of arrhythmias in AT1R mice is in support of a ventricular origin for the observed arrhythmias. However, we cannot exclude the possibility that conduction abnormalities could also contribute to some rhythm disturbances seen in these animals. Additional experimental studies are required to address this question.

In conclusion, data presented here reveal that overexpression of the human AT1R in the myocardium leads to an increased incidence of cardiac arrhythmia associated with delayed repolarization in mice. Importantly, these changes occurred before the development of cardiac remodelling and in absence of hypertension. These studies provide new insight into the role of chronic AT1R stimulation in the pathogenesis of cardiac arrhythmia and sudden death. These results could help to develop and understand therapeutic strategies preventing arrhythmic mortality associated with heart disease.

Supplementary material

Supplementary material is available at *Cardiovascular Research* online.

Acknowledgements

The authors are thankful to M.A. Lupien, M.A. Gillis, and M. Laprise for skilled technical assistance and to Hao Wang for the measurements of the AT1R levels.

Conflict of interest: none declared.

Funding

This study was supported by an operating grant from the Canadian Institutes of Health Research (MOP-64621; CF). K.R. has a studentship award from the Fonds de la Recherche en Santé du Québec (FRSQ). C.F. is a Research Scholar of the FRSQ.

References

- Flesch M, Hoper A, Dell'Italia L, Evans K, Bond R, Peshock R *et al*. Activation and functional significance of the renin-angiotensin system in mice with cardiac restricted overexpression of tumor necrosis factor. *Circulation* 2003; **108**:598–604.
- Nakamura K, Fushimi K, Kouchi H, Mihara K, Miyazaki M, Ohe T *et al*. Inhibitory effects of antioxidants on neonatal rat cardiac myocyte hypertrophy induced by tumor necrosis factor- α and angiotensin II. *Circulation* 1998; **98**:794–799.
- Akar FG, Spragg DD, Tunin RS, Kass DA, Tomaselli GF. Mechanisms underlying conduction slowing and arrhythmogenesis in nonischemic dilated cardiomyopathy. *Circ Res* 2004; **95**:717–725.
- Zhang C, Yasuno S, Kuwahara K, Zankov DP, Kobori A, Makiyama T *et al*. Blockade of angiotensin II type 1 receptor improves the arrhythmia morbidity in mice with left ventricular hypertrophy. *Circ J* 2006; **70**:335–341.
- Rials SJ, Wu Y, Xu X, Filart RA, Marinchak RA, Kowey PR. Regression of left ventricular hypertrophy with captopril restores normal ventricular action potential duration, dispersion of refractoriness, and vulnerability to inducible ventricular fibrillation. *Circulation* 1997; **96**:1330–1336.
- de Gasparo M, Catt KJ, Inagami T, Wright JW, Unger T. International union of pharmacology. XXIII. The angiotensin II receptors. *Pharmacol Rev* 2000; **52**:415–472.
- Molkentin JD, Lu JR, Antos CL, Markham B, Richardson J, Robbins J *et al*. A calcineurin-dependent transcriptional pathway for cardiac hypertrophy. *Cell* 1998; **93**:215–228.
- Molkentin JD. Calcineurin and beyond: cardiac hypertrophic signaling. *Circ Res* 2000; **87**:731–738.
- Wang Z, Kutschke W, Richardson KE, Karimi M, Hill JA. Electrical remodeling in pressure-overload cardiac hypertrophy: role of calcineurin. *Circulation* 2001; **104**:1657–1663.
- Paradis P, Dali-Youcef N, Paradis F, Thibault G, Nemer M. Overexpression of angiotensin II type 1 receptor in cardiomyocytes induces cardiac hypertrophy and remodeling. *Proc Natl Acad Sci USA* 2000; **97**:931–936.
- Pitt B, Segal R, Martinez FA, Meurers G, Cowley AJ, Thomas I *et al*. Randomised trial of losartan versus captopril in patients over 65 with heart failure (Evaluation of Losartan in the Elderly Study, ELITE). *The Lancet* 1997; **349**:747–752.
- Ricard P, Danilo P Jr, Cohen IS, Burkhoff D, Rosen MR. A role for the renin-angiotensin system in the evolution of cardiac memory. *J Cardiovasc Electrophysiol* 1999; **10**:545–551.
- Domenighetti AA, Boixel C, Cefai D, Abriel H, Pedrazzini T. Chronic angiotensin II stimulation in the heart produces an acquired long QT syndrome associated with IK1 potassium current downregulation. *J Mol Cell Cardiol* 2007; **42**:63–70.
- Mazzolai L, Nussberger J, Aubert JF, Brunner DB, Gabbiani G, Brunner HR *et al*. Blood pressure-independent cardiac hypertrophy induced by locally activated renin-angiotensin system. *Hypertension* 1998; **31**:1324–1330.
- Xiao HD, Fuchs S, Campbell DJ, Lewis W, Dudley SC Jr, Kasi VS *et al*. Mice with cardiac-restricted angiotensin-converting enzyme (ACE) have atrial enlargement, cardiac arrhythmia, and sudden death. *Am J Pathol* 2004; **165**:1019–1032.
- Zhai P, Yamamoto M, Galeotti J, Liu J, Masurekar M, Thaisz J *et al*. Cardiac-specific overexpression of AT1 receptor mutant lacking Galphaq/Galpai coupling causes hypertrophy and bradycardia in transgenic mice. *J Clin Invest* 2005; **115**:3045–3056.
- Donoghue M, Wakimoto H, Maguire CT, Acton S, Hales P, Stagliano N *et al*. Heart block, ventricular tachycardia, and sudden death in ACE2 transgenic mice with downregulated connexins. *J Mol Cell Cardiol* 2003; **35**:1043–1053.
- Trépanier-Boulay V, St-Michel C, Tremblay A, Fiset C. Gender-based differences in cardiac repolarization in mouse ventricle. *Circ Res* 2001; **89**:437–444.
- Brouillette J, Clark RB, Giles WR, Fiset C. Functional properties of K⁺ currents in adult mouse ventricular myocytes. *J Physiol* 2004; **559**:777–798.
- Mitchell GF, Jeron A, Koren G. Measurement of heart rate and QT interval in the conscious mouse. *Am J Physiol* 1998; **274**:H747–H751.
- Lizotte E, Tremblay A, Allen BG, Fiset C. Isolation and characterization of subcellular protein fractions from mouse heart. *Anal Biochem* 2005; **345**:47–54.
- Grandy SA, Trépanier-Boulay V, Fiset C. Postnatal development has a marked effect on ventricular repolarization in mice. *Am J Physiol* 2007; **293**:H2168–H2177.
- Aries A, Paradis P, Lefebvre C, Schwartz RJ, Nemer M. Essential role of GATA-4 in cell survival and drug-induced cardiotoxicity. *Proc Natl Acad Sci USA* 2004; **101**:6975–6980.
- Wickenden AD, Lee P, Sah R, Huang Q, Fishman GI, Backx PH. Targeted expression of a dominant-negative Kv4.2 K⁺ channel subunit in the mouse heart. *Circ Res* 1999; **85**:1067–1076.
- Barry DM, Xu H, Schuessler RB, Nerbonne JM. Functional knockout of the transient outward current, long-QT syndrome, and cardiac remodelling in mice expressing a dominant-negative Kv4 α -subunit. *Circ Res* 1998; **83**:560–567.

26. Xu H, Barry DM, Li H, Brunet S, Guo W, Nerbonne JM. Attenuation of the slow component of delayed rectification, action potential prolongation, and triggered activity in mice expressing a dominant-negative Kv2 alpha-subunit. *Circ Res* 1999;**85**:623–633.
27. Zaritsky JJ, Redell JB, Tempel BL, Schwarz TL. The consequences of disrupting cardiac inwardly rectifying K⁺ current (I_{K1}) as revealed by the targeted deletion of the murine Kir2.1 and Kir2.2 genes. *J Physiol* 2001;**533**: 697–710.
28. Beuckelmann DJ, Nabauer M, Erdmann E. Alterations of K⁺ currents in isolated human ventricular myocytes from patients with terminal heart failure. *Circ Res* 1993;**73**:379–385.
29. Kaab S, Nuss HB, Chiamvimonvat N, O'Rourke B, Pak PH, Kass DA *et al.* Ionic mechanisms of action potential prolongation in ventricular myocytes from dogs with pacing-induced heart failure. *Circ Res* 1996;**78**: 262–273.
30. Priebe L, Beuckelmann DJ. Simulation study of cellular electric properties in heart failure. *Circ Res* 1998;**82**:1206–1223.
31. London B, Guo W, Pan X, Lee JS, Shusterman V, Rocco CJ *et al.* Targeted replacement of KV1.5 in the mouse leads to loss of the 4-aminopyridine-sensitive component of I(K,slow) and resistance to drug-induced qt prolongation. *Circ Res* 2001;**88**:940–946.
32. Zhou J, Kodirov S, Murata M, Buckett PD, Nerbonne JM, Koren G. Regional upregulation of Kv2.1-encoded current, I_{K,slow2}, in Kv1DN mice is abolished by crossbreeding with Kv2DN mice. *Am J Physiol Heart Circ Physiol* 2003;**284**:H491–H500.
33. Fischer R, Dechend R, Gapelyuk A, Shagdarsuren E, Gruner K, Gruner A *et al.* Angiotensin II-induced sudden arrhythmic death and electrical remodeling. *Am J Physiol* 2007; 01400.
34. Hayabuchi Y, Davies NW, Standen NB. Angiotensin II inhibits rat arterial KATP channels by inhibiting steady-state protein kinase A activity and activating protein kinase C ϵ . *J Physiol* 2001;**530**:193–205.
35. Toro L, Amador M, Stefani E. ANG II inhibits calcium-activated potassium channels from coronary smooth muscle in lipid bilayers. *Am J Physiol* 1990;**258**:H912–H915.
36. Clement-Chomienne O, Walsh MP, Cole WC. Angiotensin II activation of protein kinase C decreases delayed rectifier K⁺ current in rabbit vascular myocytes. *J Physiol* 1996;**495**:689–700.
37. Zhang TT, Takimoto K, Stewart AFR, Zhu C, Levitan ES. Independent regulation of cardiac Kv4.3 potassium channel expression by angiotensin II and phenylephrine. *Circ Res* 2001;**88**:476–482.
38. Yu H, Gao J, Wang H, Wymore R, Steinberg S, McKinnon D *et al.* Effects of the renin-angiotensin system on the current I(to) in epicardial and endocardial ventricular myocytes from the canine heart. *Circ Res* 2000;**86**: 1062–1068.
39. Shimoni Y. Inhibition of the formation or action of angiotensin II reverses attenuated K⁺ currents in type 1 and type 2 diabetes. *J Physiol* 2001; **537**:83–92.

ON LINE DATA SUPPLEMENT

Cardiac-specific overexpression of the human type 1 angiotensin II receptor causes delayed repolarization **Rivard *et al.***

Ventricular myocytes isolation

CTL and AT1R mice were heparinized (1 U/kg; IP) 20 min prior to sacrifice, anaesthetized by inhalation with isoflurane and then killed by cervical dislocation. The hearts were rapidly removed, and retrogradely perfused (2 ml/min) through the aorta on a modified Langendorff apparatus with the following solutions: (i) 5 minutes with HEPES-buffered Tyrode solution containing (in mM): 130 NaCl; 5.4 KCl; 1 CaCl₂; 1 MgCl₂; 0.3 Na₂HPO₄; 10 HEPES; 5.5 glucose (pH adjusted to 7.4 with NaOH), (ii) 10 min with Tyrode solution without Ca²⁺ (“Ca²⁺-free”), (iii) 20 min with Ca²⁺-free Tyrode solution containing 73.7 U ml⁻¹ collagenase type 2 (Worthington Co. Ltd, Freehold, NJ, USA); 0.1% bovine serum albumin (BSA; Fraction V, Sigma Chemicals Co., St. Louis, Mo, USA); 20 mM taurine and 30 μM CaCl₂, and (iv) 5 min 30 sec with a “KB” solution¹ containing (in mM): 100 K⁺-glutamate; 10 K⁺-aspartate; 25 KCl; 10 KH₂PO₄; 2 MgSO₄; 20 taurine; 5 creatine base; 0.5 EGTA; 5 HEPES; 0.1% BSA; 20 glucose (pH adjusted to 7.2 with KOH). The temperature of the perfusion was maintained at 37±1 °C. At the end of the perfusion, the right ventricular free wall was dissected from the heart and placed in KB solution. The tissue was then minced and titrated for 10 min to free individual ventricular myocytes. Myocytes were stored in KB solution at 4 °C until needed.

Electrophysiology

Cellular electrophysiology. Whole-cell voltage and current-clamp recordings were performed on the myocytes using ruptured patch technique with a patch-clamp amplifier, Axopatch 200 B

(Axon Instruments, Foster City, USA) and data were recorded and analyzed with pClamp 8.0 software (Axon Instruments, Foster City, USA). Cells were continuously perfused with oxygenated Tyrode solution containing (in mM): 130 NaCl; 5.4 KCl; 1 CaCl₂; 1 MgCl₂; 0.3 Na₂HPO₄; 10 HEPES; 5.5 glucose (pH adjusted to 7.4 with NaOH). Pipettes had resistances between 1.5-3.5 MΩ when filled with the following solution (mM): 110 K⁺-aspartate, 20 KCl, 8 NaCl, 1 MgCl₂, 1 CaCl₂, 10 BAPTA, 4 K₂ATP and 10 HEPES (pH 7.2 with KOH). Series resistance (R_s) was between 4-8 MΩ; and compensation was applied to reduce R_s by 80-90%. Voltage-clamp currents were low-pass filtered at 1 kHz with a 4-pole Bessel analog filter, digitized at 4-10 kHz. To account for differences in cell size, current amplitudes were normalized to the cell capacitance, and expressed as densities (pA/pF). Capacitive transients elicited by a 10 mV depolarizing step from a holding potential of -80 mV were recorded at 25 kHz (filtered at 10 kHz). Cell capacitance was measured by integrating the surface area of these capacitive transient. To compensate for the patch pipette-bath liquid junction potential (K⁺-Aspartate) recorded membrane potentials were corrected by -10 mV. All experiments were carried out at room temperature (20-22°C).

K⁺ currents recordings. Current-voltage relationship for the total K⁺ current (I_{peak}) was constructed from the current elicited by a series of 500 ms test potentials varying from -110 mV to +50 mV in 10 mV increments from a holding potential of -80 mV at a frequency rate of 0.1 Hz. We then examined the contribution of individual outward K⁺ currents: I_{to}, I_{Kur} and I_{ss}. First, we eliminated the transient portion (or I_{to}) by applying an inactivating prepulse (100 ms, -40 mV) preceding the main activation steps. We then compared the density of I_{to} obtained by subtracting the current traces measured with and without the inactivating prepulse. The current remaining after inactivation of I_{to} is denoted I_{Kslow} and is composed of I_{Kur} (or the 4-

aminopyridine (4-AP)-sensitive component) and I_{ss} (or the 4-AP-resistant component). To measure I_{ss} , we applied 100 μ M 4-AP (which blocks I_{Kur}) in combination with an inactivating prepulse (which blocks I_{to}) and then recorded I_{ss} . We measured I_{Kur} by subtracting currents recorded in absence or presence of 4-AP ($I_{Kslow} - I_{ss}$). The description and validation of these pharmacological and biophysical methods has been recently published².

K^+ currents were recorded in absence of sodium or L-type Ca^{2+} currents blockers to allow recordings of K^+ currents and action potentials from the same myocyte. Under our recording conditions (room temperature, presence of BAPTA in the intracellular solution), I_{Ca} are small. Also, the intrinsic very fast activation and inactivation of I_{Na} prevent interference of this current with K^+ currents (I_{Na} activates and inactivates before K^+ currents fully activate).

Steady-state inactivation. The voltage-dependence of steady-state inactivation for I_{to} and I_{Kur} were measured using two-step voltage-clamp protocol. The first step is an inactivating pulse to selected potential (from -110 to -10 mV) maintained for a period of 1 s or 5 s, for I_{to} and I_{Kur} , respectively. This inactivating pulse is followed by a second voltage step to +30 mV during 1 s (I_{to}) or 5 s (I_{Kur}) (See figure inset for voltage protocols). For the I_{Kur} recording, a pulse at -40 mV for 100 ms had been added between the inactivating and test pulse to inactivate I_{to} . Both I_{to} and I_{Kur} currents amplitude at each pulse potential were normalized to the maximum amplitude of each family of current (I/I_{max}) and plotted as a function of the inactivating pre-pulse potential. Data were fit to a Boltzmann equation : $I/I_{max} = 1 / [1 + \exp((V_m - V_{1/2})/S_{1/2})]$, where $V_{1/2}$ represents the membrane potential (V_m) at which 50% of the channels are inactivated and $S_{1/2}$, is the mid-point slope factor (mV).

Recovery from inactivation. To measure the time dependence for reactivation of I_{to} and I_{Kur} , an inactivating pulse (at +30 mV, maintain for 500 ms and 1.5 s period for I_{to} and I_{Kur} respectively) was followed at variable time intervals by a test pulse (at +30 mV for 500 ms for both types of current) (Protocols are shown in figure inset). The interpulse period varied between 10 and 600 ms for I_{to} recording and between 50 ms and 3 s for I_{Kur} . Specifically to I_{Kur} , both inactivating and test pulse were preceded by a pulse of 100 ms at -40 mV to inactivate I_{to} . I_{Kur} amplitude was measured by subtraction amplitude of outward current at the peak and 500 ms after the peak. For both families of current, the holding and interpulse potentials were -80 mV. Analysis of the recovery from inactivation was made using P2/P1 ratio plotted as a function of interpulse time and time constant was calculated (ms). P2 represents current amplitude of the test pulse and P1 corresponds to the inactivating pulse.

Action potential recordings. Action potentials were recorded at frequency rates of 1 to 4 Hz with the whole-cell current-clamp protocol by injection of brief (1-3 ms) stimulus currents (0.4-0.7 nA). The action potential durations of control and AT1R mouse ventricular myocytes were measured at 20, 50 and 90% of repolarization.

Surface electrocardiogram (ECG). Mice were anaesthetized with isoflurane. Mouse body temperature was maintained at 37°C using a heating pad. Platine electrodes were placed subcutaneous and surface ECG was acquired in lead I configuration. Acquisition was performed using the Biopac System MP100 at a rate of 2 kHz. The signal was amplified, filtered at 100 Hz (low-pass) and 60 KHz (notch filter). Data were analyzed using ECG auto 1.5.³ The QT intervals and other ECG parameters were measured by two blinded observers from signal averaged ECG recordings.

Telemetry recording. Data was acquired with an implantable OpenHeart® radiofrequency transmitter, (Data Sciences International, Arden Hills, MN). Individual transmitters were implanted into a right lateral abdominal subcutaneous pouch of CTL and AT1R mice (6-8 months, n=6 per group; 50 days, n=4 CTL and 3 AT1R). ECG lead placement represented the lead II configuration. All mice were allowed to recover for 1 week after surgery. ECG were continuously recorded for a period of 24 hours and saved onto disk for later analysis. Recordings were analyzed with ECG Auto (version 1.5, EMKA technologies, Paris, France).⁴

Western blots analysis

Proteins were prepared from ventricles of CTL and AT1R mice (1 heart/sample). Protein (100 µg/lane) were separated by SDS polyacrylamide gel electrophoresis and transferred on PVDF membranes and assayed for K⁺ channels expression by Western blot. Rabbit polyclonal primary antibodies directed against Kv1.5 (1:500), Kv2.1 (1:500), Kv4.2 (1:1000), Kv4.3 (1:1000) and Kir2.1 (1:500) were used. All antibodies were purchased from Alomone Labs (Jerusalem, Israel), with the exception of Kv1.5, which was obtained from Upstate Biotechnology (Lake Placid, NY, USA). Bands were quantified by densitometry using Multi-Analyst program (Bio-Rad, Ca, USA).

Real time PCR

Total RNA was isolated from CTL and AT1R ventricles using RNeasy Fibrous Tissue kit (Qiagen) and treated with DNase I. cDNA fragments were synthesized by RT using the cloned AMV reverse transcriptase (InVitrogen). Primers specific to each K⁺ channel studied (Kv1.5, Kv2.1, Kv4.2, Kir2.1 and KChIP2) were designed, tested by real-time PCR and a melting curve was performed to assure an amplification of a unique cDNA product. Sequence analysis was

performed on all PCR-generated cDNA fragments to ascertain the specificity of the products. The real-time PCR reaction was carried out with Platinum SYBR Green qPCR Supermix (Invitrogen) using a real-time PCR system (MX3005P QPCR system, Stratagene). The PCR reactions were cycled 40 times using a 3-step cycle procedure (denaturation at 95°C for 30s, annealing at 50°C for 45s, elongation at 72°C for 45s) after an initial stage at 95°C for 10 min to activate the Taq polymerase. mRNA expression was quantified relative to the murine cyclophilin. mRNA expression was quantified by measuring fluorescence intensities at the beginning of the linear region of the fluorescence versus cycle number curves (amplification curves).

Echocardiography

Two-dimensional guided M-mode echocardiography was performed under conscious sedation with 10 µL/g i.p. of 1:1 mixture of Fentanyl (5 µg /ml) and Droperidol (250 µg/ml) using a Philips Sonos 5500 and a 15-MHz linear-array transducer. The mice were lightly secured in the left lateral decubitus position on a warming pad to maintain normothermia. To improve the nearfield image for visualization of the interventricular septum, a standoff constituted of a 3 to 5 mm thick 1% agarose pad, was inserted between the chest of the mice and the transducer. The montage was acoustically sealed with prewarm acoustic coupling gel. Fractional shortening (FS) and left ventricular mass (LV mass) were determined.

REFERENCES

1. Isenberg G, Klockner U. Calcium tolerant ventricular myocytes prepared by preincubation in a "KB medium". *Pflug Arch* 1982;**395**:6-18.
2. Brouillette J, Clark RB, Giles WR, Fiset C. Functional properties of K⁺ currents in adult mouse ventricular myocytes. *J Physiol* 2004;**559**:777-798.
3. Brouillette J, Trepanier-Boulay V, Fiset C. Effect of androgen deficiency on mouse ventricular repolarization. *J Physiol* 2003;**546**:403-413.
4. Brouillette J, Grandy SA, Jolicoeur P, Fiset C. Cardiac repolarization is prolonged in CD4C/HIV transgenic mice. *J Mol Cell Cardiol* 2007;**43**:159-167.